END
8-87
DTIC

②

AD-A181 925

CUMENTATION PAGE | READ INSTRUCTIONS BEFORE COMPLETING FORM

AFOSR-TR. 87-0799

	2. GOVT ACCESSION NO.	1. RECIPIENT'S CATALOG NUMBER

4. TITLE (and Subtitle)	5. TYPE OF REPORT & PERIOD COVERED
Spline-Based Parameter Estimation Techniques for Two-Dimensional Convection and Diffusion Equations	
	6. PERFORMING ORG. REPORT NUMBER

7. AUTHOR(s)	8. CONTRACT OR GRANT NUMBER(s)
L.L. Zia	AFOSR-84-0398

9. PERFORMING ORGANIZATION NAME AND ADDRESS	10. PROGRAM ELEMENT, PROJECT, TASK AREA & WORK UNIT NUMBERS
Lefschetz Center for Dynamical Systems Division of Applied Mathematics Brown University, Providence, RI 02912	61102F 2304 A1

11. CONTROLLING OFFICE NAME AND ADDRESS	12. REPORT DATE
Air Force Office of Scientific Research Bolling Air Force Base Washington, DC 20332	July, 1986
	13. NUMBER OF PAGES
	48

14. MONITORING AGENCY NAME & ADDRESS(if different from Controlling Office)	15. SECURITY CLASS. (of this report)
SAme as 11	Unclassified
	15a. DECLASSIFICATION/DOWNGRADING SCHEDULE

16. DISTRIBUTION STATEMENT (of this Report)

Approved for public release: distribution unlimited

17. DISTRIBUTION STATEMENT (of the abstract entered in Block 20, if different from Report)

18. SUPPLEMENTARY NOTES

19. KEY WORDS (Continue on reverse side if necessary and identify by block number)

Parameter estimation, distributed parameter systems, convection and diffusion

20. ABSTRACT (Continue on reverse side if necessary and identify by block number)

INCLUDED — on reverse

20. Abstract

A general approximation framework based on bicubic splines is developed for estimating temporally and spatially varying parameters in two-dimensional convection and diffusion equations derived from mass transport theory. The "parameter estimation problem" is first cast as an abstract infinite dimensional minimization problem. Then a sequence of approximate, finite dimensional minimization problems is defined, which yields a sequence of parameter estimates. Convergence results relating the approximate problems to the full infinite dimensional problem are presented, as well as a discussion addressing computer implementation. Finally, the technique is applied to the analysis of actual biological data from an insect dispersal experiment, in which the movement of cabbage root flies in the presence of a cabbage crop was studied. It is proposed that such a parameter estimation method can be a useful analytical tool to help develop appropriate models in population biology.

Accession For	
NTIS GRA&I	☒
DTIC TAB	☐
Unannounced	☐
Justification	
By	
Distribution/	
Availability Codes	
Dist	Avail and/or Special
A-1	

SPLINE-BASED PARAMETER ESTIMATION
TECHNIQUES FOR TWO-DIMENSIONAL
CONVECTION AND DIFFUSION EQUATIONS

by

L.L. Zia

July 1986

LCDS T^{12} #86-46

Lefschetz Center for Dynamical Systems

Division of Applied Mathematics   Brown University Providence RI 02912

SPLINE-BASED PARAMETER ESTIMATION TECHNIQUES FOR TWO-DIMENSIONAL CONVECTION AND DIFFUSION EQUATIONS

by

L.L. Zia

July 1986

LCDS-#86-46

SPLINE-BASED PARAMETER ESTIMATION

TECHNIQUES FOR TWO-DIMENSIONAL

CONVECTION AND DIFFUSION EQUATIONS

L.L. Zia

Department of Mathematics

University of New Hampshire

Durham, NH   03824

July 1986

SPLINE-BASED PARAMETER ESTIMATION

TECHNIQUES FOR TWO-DIMENSIONAL

CONVECTION AND DIFFUSION EQUATIONS

L.L. Zia

ABSTRACT

A general approximation framework based on bicubic splines is
developed for estimating temporally and spatially varying parameters in
two-dimensional convection and diffusion equations derived from mass transport
theory. The "parameter estimation problem" is first cast as an abstract
infinite dimensional minimization problem. Then a sequence of approximate,
finite dimensional minimization problems is defined, which yields a sequence
of parameter estimates. Convergence results relating the approximate problems
to the full infinite dimensional problem are presented, as well as a
discussion addressing computer implementation. Finally, the technique is
applied to the analysis of actual biological data from an insect dispersal
experiment, in which the movement of cabbage root flies in the presence of a
cabbage crop was studied. It is proposed that such a parameter estimation
method can be a useful analytical tool to help develop appropriate models in
population biology.

I. Introduction

When constructing a mathematical model, one often finds it desirable to estimate unknown parameters in that model based on actual observations of the particular phenomenon under study. In the transport equations used by mathematical ecologists to model population dispersal, one typically seeks estimates of parameters representing diffusion, convection and "growth/death" rates. Recognizing that these models are very naturally posed on a two-dimensional domain, we develop a bicubic spline based parameter estimation technique for a general two-dimensional transport equation. Our efforts are guided by two important considerations: one, the necessity for a computationally efficient procedure and two, a guarantee that such a procedure will yield a set of parameter estimates that is "optimal" in some sense.

In Section II we give a precise mathematical formulation of what we mean by an estimation problem. It will be seen that such a problem is infinite dimensional in nature and thus difficult to solve; so one is led quite naturally to define a sequence of finite dimensional "approximate estimation problems" in an attempt to obtain a solution. A theorem is presented relating this sequence of approximations to the full estimation problem, and the result serves to clarify the sense of "optimality" alluded to above. The actual implementation of the approximation technique formulated in Section II will be described in Section III and numerical examples will be given. Finally, in Section IV, we present the results of an analysis of real biological data.

Throughout this report we shall adopt the following conventions. Differentiation of a function, u, with respect to t, x, and y will be denoted by u_t, u_x, and u_y, respectively, with obvious extensions to higher order derivatives. The symbol $\otimes$ will stand for the Kronecker product. We will let

$L^2 = L^2(\Omega)$ be the usual Hilbert space of square integrable functions on Ω, a bounded domain of R^2, with norm $|| \cdot ||_0$ and inner product $\langle \cdot, \cdot \rangle$. Likewise, $L^\infty = L^\infty(\Omega)$ will be the usual Banach space of essentially bounded functions with norm $|| \cdot ||_\infty$. We will denote by $H^i(\Omega)$, $i = 0,1,2,\ldots$, the Sobolev spaces with norm $|| \cdot ||_i$ of "functions" in $L^2(\Omega)$ whose i^{th} "derivative" is also in $L^2(\Omega)$. Furthermore $H_0^i(\Omega)$, $i = 1,2,\ldots$, will be the Sobolev space of elements of $H^i(\Omega)$ whose "derivatives" of order up to i-1 vanish on $\partial\Omega$, the boundary of Ω. Finally, we will often use the terms parameter and coefficient interchangeably, as well as estimation and identification.

II. Mathematical formulation

We consider the initial value-boundary value problem (IV-BVP) on $\Omega = [0,1] \times [0,1]$:

$$u_t + \nabla\cdot(Vu) = \nabla\cdot(D \times \nabla u) + \alpha u + f, \qquad t\varepsilon(0,T],$$

(2.1) $$u(0,x,y) = u_0(\gamma(x,y)),$$

$$u(t,x,y) = 0 \text{ on } \partial\Omega,$$

where $f = f(\beta,t,x,y)$ and D, V, α, and β are assumed to be functions of t, x, and y, with $D = (D_1,D_2)$ with $V = (v_1,v_2)$. The dependent variable, $u = u(t,x,y)$, represents the population density of a species, whose dispersal over a two-dimensional domain is assumed to result from an innate diffusive mechanism, D, and a convective or "directed transport" mechanism, V. The parameter α represents a general "source/sink" or "growth/death" term. (For the definitive account of diffusion models in ecology we cite the excellent book by Okubo [13]). Without loss of generality we have assumed homogeneous Dirichlet boundary conditions, since any non-homogeneous boundary conditions, with possibly unknown parameters, can be included in the parameters β and γ via a standard transformation. In fact, if we had the boundary condition u =

F on $\partial\Omega$, then we could define a new dependent variable to be $v = u - g(x,y)\cdot F$ where $g(x,y) = 1 - xy(1 - x)(1 - y)$. Substituting this transformation into (2.1) to get an equation for v, we see that we must assume the inhomogeneous term F is C^1 in t, and C^2 in x and y. Notice however, that $g(x,y) = 1$ on $\partial\Omega$ so that $v(t,x,y) = 0$ on $\partial\Omega$. Finally we note that solutions to (2.1) will be considered in the sense of distributions so that we can use the abstract framework of Lions [12] and invoke weak variational theory to discuss the well-posedness of this IV-BVP.

Let q be a "vector" of parameters $(D,V,\alpha,\beta,\gamma)$. Dropping the Kronecker product symbol $\otimes$ for ease of notation, we define the bilinear form $L(q)$: $H_0^1(\Omega) \times H_0^1(\Omega) \to R$ by:

$$(2.2) \qquad L(q)(\phi,\psi) = \langle D\nabla\phi, \nabla\psi\rangle - \langle V\phi, \nabla\psi\rangle - \langle\alpha\phi, \psi\rangle$$

and then rewrite (2.1) in its weak form in the state space $L^2(\Omega)$:

$$(2.3) \qquad \begin{aligned} &\langle u_t, \phi\rangle + L(q)(u,\phi) = \langle f,\phi\rangle, \text{ for all } \phi \text{ in } H_0^1(\Omega), \\ &u(0) = u_0(\gamma), \end{aligned}$$

where $\langle\cdot,\cdot\rangle$ is the standard L^2 inner product on $[0,1] \times [0,1]$. Note that the boundary conditions have been incorporated into the equation of state.

We assume throughout that q belongs to some set Q of admissible parameter functions that is compact in the space: $X = \{H^1([0,T];L^2(\Omega))\}^2 \times \{H^0((0,T) \times \Omega)\}^3$. Furthermore we make the following assumptions:

(A1)   Q is a bounded subset of $\{L^\infty([0,T] \times \Omega)\}^5$, with the bound m_2;

(A2)   There exists $m_1 > 0$ such that for any $q \in Q$, the components of D satisfy $D_i \geq m_1$, $i = 1,2$ for all t, x, and y;

(A3)   The inhomogeneous term f is C^1 in all of its arguments, the initial data u_0 belongs to $H^2(\Omega)$, and the map $\gamma \to u_0(\gamma)$ is continuous from $L^2(\Omega)$ to $H^2(\Omega)$;

(A4)   For any q in Q, D_t and $V_t \in Q_1$, a bounded subset of $L^\infty([0,T] \times \Omega)$ with the bound m_3.

Theorem 2.1: Under the assumptions (A1), (A2), and (A3), the initial value problem (2.3) has a unique weak solution $u(t,\cdot,\cdot;q) \in H_0^1(\Omega)$. Furthermore this weak solution depends continuously on the initial data u_0.

Proof: We appeal directly to the weak variational theory of Lions, pp. 100-111, [12]. ///

With the state equation (2.3) in hand we now assume that for each time t_i in $(0,T]$, $i = 1,\ldots,P$ we are given a matrix $\Lambda(t_i)$ of observations (taken at the m·n locations $(x_1,y_1),\ldots,(x_m,y_n)$). Associated with each $\Lambda(t_i)$ is a matrix $\Gamma(t_i;q) = (u(t_i,x_j,y_k;q))$ of model based "predictions", obtained by evaluating the q-dependent solution u at the points (x_j,y_k) $1 \le j \le m$ and $1 \le k \le n$. Using this information we seek a vector of parameters, q, that will yield the "best fit" of the model to the data. Thus, we formulate the parameter estimation problem as follows:

$$(2.4) \qquad \text{minimize } J(q) = \sum_{i=1}^{P} || \Lambda(t_i) - \Gamma(t_i;q) ||^2$$

over all q belonging to the set of admissible parameter functions, Q. Here the norm is taken to be the Euclidean norm in the space R^{mn} and it is clear that $J(q)$ is a pointwise least squares cost functional.

An unavoidable difficulty now arises, for the minimization problem we have formulated is inherently an infinite dimensional one and thus hard to

solve. Indeed, we must always contend with the infinite dimensionality of the state, $u(t,\cdot,\cdot;q)$, when we try to solve (2.3); and if we also consider variable coefficients, we must then deal with a minimization over an infinite dimensional set of parameters. Because we usually cannot solve equation (2.3) exactly, we would like instead to compute an approximate solution to (2.3) and thus generate a matrix of "approximate predictions" to use in the cost functional J. We would also like to employ a similar strategy to reduce the infinite dimensional minimization problem to a sequence of finite dimensional minimizations. Since approximation schemes for these two cases will be essentially independent of one another [2], it will greatly simplify our notation if we focus first on the approximation of the state space and postpone discussion of the parameter set approximation.

Galerkin schemes based on cubic splines are already well developed for approximating solutions to transport equations on a one-dimensional domain [1], [2], [3], [4], [5] and these are readily extended to two-dimensional domains. Following the standard Galerkin technique, we define a sequence of finite dimensional approximating state subspaces $H^N \subset L^2$, $N = 1,2,\ldots$, with $P^N: L^2 \to H^N$ the canonical orthogonal projection. Furthermore, we assume that $H^N \subset H_0^1(\Omega)$ and that:

(B)   For all $z \in C^2(\Omega) \cap H_0^1(\Omega)$, $||P^N z - z||_0$ and $||\nabla(P^N z - z)||_0$

        are less than or equal to $\varepsilon(N)\{||z_{xx}||_0 + ||z_{yy}||_0\}$ where

        $\varepsilon(N) \to 0$ as $N \to \infty$.

We remark that by using arguments from Chapter 6 of [14] and pp. 17-18 of [6], it can be seen that a finite element approximation scheme based on bicubic splines satisfies these conditions. In addition, the following L^∞ convergence rate can be shown to hold: $||P^N z - z||_\infty \leq (c/N^2)\{||z_{xx}||_\infty + ||z_{yy}||_\infty\}$.

Restricting the bilinear form (2.2) to $H^N \times H^N$, we then define the Galerkin approximation, $u^N = u^N(t, \cdot, \cdot; q)$ to be the solution of:

(2.5)
$$\langle u_t^N, \psi \rangle + L(q)(u^N, \psi) = \langle f, \psi \rangle, \text{ for all } \psi \text{ in } H^N,$$
$$u^N(0) = P^N u_0.$$

We note that we can view this equation as the result of projecting equation (2.3) into the finite dimensional subspace H^N, and as such (2.5) inherits the well-posedness of its parent equation.

Theorem 2.2: Under the assumptions (A1), (A2), and (A3), the initial value problem (2.5) has a unique weak solution $u^N(t, \cdot, \cdot; q)$, belonging to $H^N(\Omega)$ and depending continuously on the initial data. In fact, given the finite dimensionality of the equation, u^N is a strong solution.

Proof: As before, we appeal directly to the theory of Lions, pp. 100-111, [12]. ///

Having defined a sequence of equations approximating (2.3), we can define a sequence of approximate estimation problems as follows:

(2.6)
$$\text{minimize } J^N(q) = \sum_{i=1}^{P} || \Lambda(t_i) - u^N(t_i, x_j, y_k, q) ||^2$$

over all q belonging to the set of admissible parameter functions, Q. We note however, that (2.6) is still an infinite dimensional problem, and this fact leads us to discuss the approximation of the parameter set Q.

In a manner similar to that for the state approximation scheme we define a sequence Q^M of finite dimensional sets that approximate Q in a certain sense. Recall that we have defined X to be the space: $\{H^1([0,T]; L^2(\Omega))\}^2 \times \{H^0((0,T) \times \Omega)\}^3$. Then, following the ideas developed in

[2], we let Q^M, $M = 1,2,\ldots$, be subsets of X defined by $Q^M = i^M(Q)$, where i^M:
$Q \subset X \to X$. In addition we assume:

(C1)   The mappings i^M: $Q \to X$ are continuous;

(C2)   For each $q \in Q$, $i^M(q) \to q$ as $M \to \infty$, uniformly in Q.

We observe here that in Section III we shall discuss an approximation scheme
for Q based on linear splines, and it can be shown that such a scheme
satisfies the above assumptions. In fact we will take the mappings i^M to be
the Mth order interpolating linear spline operator. That is for $q \in Q$:

$$i^M(q) = \sum q(t_i, x_j, y_k)\delta_i(t)\lambda_j(x)\nu_k(y) \quad i,j,k = 0,1,\ldots,M$$

where δ_i, λ_j, and ν_k are the standard linear splines defined on equal
partitions of $[0,T]$, $[0,1]$, and $[0,1]$ with mesh sizes T/M, $1/M$, and $1/M$,
respectively (see [14]). With these definitions Q^M can be characterized as:

$$Q^M = \{q:[0,T] \times \Omega \to R^5 \mid q_n = \sum \sigma_{nijk}\delta_i\lambda_j\nu_k, \text{ where } \sigma_{nijk} \in \Delta_{nijk}\}.$$

Here the sum is of course taken over $i,j,k = 0,1,\ldots, M$ and Δ_{nijk} are
appropriate compact subsets of R. We also note that we have taken the same
degree of approximation, M, in each of the variables t,x, and y, but only for
illustrative purposes. For complete details of this construction see [2].

Given these approximating sets Q^M, we can now define a sequence of
finite dimensional approximate estimation problems by restricting the
minimization of J^N in (2.6) to be over the set of all q in Q^M. The following
theorem relates the solutions of these problems to a solution of the full
estimation problem (2.4).

Theorem 2.3: Let Q be compact in X. Then for each M and N, the minimization
problem (2.6) has a solution $\bar{q}_M^N$. Furthermore, there exists an element q^* of

Q and a subsequence, denoted again by $\bar{q}_M^N$, that converges to q^* in X, and this limit, q^*, is a solution to the full parameter estimation problem (2.3).

We will not present the entire proof of this theorem here, but rather will outline just the essential arguments. For complete details see [17].

Let $u^N(\cdot,q)$ be the Galerkin solution to equation (2.5). It can be shown that for each $t\varepsilon(0,T]$, the mapping $q \rightarrow u^N(t,q)$ from the set of admissible parameter functions, Q, to $L^\infty(\Omega)$ is continuous. This immediately implies the continuity of the approximate cost functionals J^N. The sets Q^M are compact since each is the image of the compact set Q under the continuous map i^M (see assumption (C1) earlier). Hence for each M and N, there exists a minimizer $\bar{q}_N^M$ of J^N over Q^M. Furthermore, by definition of the sets Q^M, there exists a sequence $\{\hat{q}_N^M\} \subset Q$ such that $\bar{q}_N^M = i^M(\hat{q}_N^M)$. Compactness of Q then implies the existence of a subsequence, which we write again as $\hat{q}_N^M$, that converges to some q^* in Q. It can then be shown that the corresponding subsequence $\bar{q}_N^M$ also converges to q^*.

Finally, to argue that q^* solves the full estimation problem (2.4) requires proving the fundamental result that "convergence of any sequence of parameters q^K to some q^* implies convergence of $J^N(q^K)$ to $J(q^*)$ as N and K $\rightarrow$ ∞". Since the cost functionals J^N and J represent <u>pointwise</u> least squares fit-to-data criteria, we see that we must guarantee <u>pointwise</u> convergence of our state approximations. That is, under an appropriate topology on Q, we must show that convergence of q^K to q^* implies $u^N(t,x_j,y_k; q^K)$ converges to $u^*(t,x_j,y_k; q^*)$ as N and K $\rightarrow \infty$, for each of the data points (x_j,y_k) $1\leq j \leq m$ and $1 \leq k \leq n$. Notice that we are not asking for global pointwise convergence of the state approximations. Rather, it will suffice to show local pointwise convergence, and then piece together at most a finite number (in fact m·n) of

such results. The arguments for this convergence rely on a general technique from finite element theory that estimates a local L^∞ norm in terms of a global H^1 norm. We then use the weak variational framework of our approximation scheme to derive inequalities from which we can obtain appropriate estimates to establish convergence in this stronger norm. For another approach to pointwise convergence in two-dimensional domains see [11].

III. Numerical implementation and examples

We turn now to a description of the implementation on the computer of the approximation framework formulated in Section II. For transport equations on a one-dimensional domain cubic spline based Galerkin schemes have been used successfully and their computational efficiency well-documented [1], [2], [3], [4], [5]. We shall see shortly that the key feature of a bicubic spline based approximation technique for two-dimensional transport equations is that the necessary computations reduce in a natural way to those computations arising in the one-dimensional problem. For notational simplicity we will illustrate this feature for the case of constant parameters, then describe the straightforward modifications needed when variable coefficients are considered.

Recall that we have defined the Galerkin approximation to our original IV-BVP to be the solution of:

$$(3.1) \quad \begin{aligned} &\langle u_t^N, \psi \rangle + \langle D \nabla u^N, \nabla \psi \rangle = \langle V u^N, \nabla \psi \rangle + \langle \alpha u^N, \psi \rangle + \langle zf, \psi \rangle \\ &u^N(0) = P^N u_0, \quad \text{for all } \psi \text{ in } H^N, \end{aligned}$$

where we have rewritten (2.5) using the definition of the bilinear form $L(q)$. We take H^N to be the span of $\{\beta_{ij}\}_{i,j=0}^N$ (where $\beta_{ij} = B_i(x)B_j(y)$ are the bicubic splines that arise as pairwise products of cubic splines B_i, corresponding to the partition $\Delta = \{i/N\}_{i=0}^N$ on $[0,1]$ and satisfying $B_i(0) = B_i(1) = 0$. Thus we can write the Galerkin approximation u^N as:

$$(3.2) \quad u^N(t) = \sum v_{ij}^N(t)\beta_{ij}(x,y) \quad i,j = 0,1,2,\ldots,N$$

where we have suppressed the dependence of β_{ij} on N. Notice that u^N automatically satisfies the homogeneous Dirichlet boundary conditions.

With this choice of the subspaces H^N, equation (3.1) is equivalent to:

(3.3)

$$\langle u_t^N, \beta_{ij} \rangle + \langle D_1 u_x^N, (\beta_{ij})_x \rangle + \langle D_2 u_y^N, (\beta_{ij})_y \rangle =$$

$$\langle v_1 u^N, (\beta_{ij})_x \rangle + \langle v_2 u^N, (\beta_{ij})_y \rangle + \langle \alpha u^N, \beta_{ij} \rangle + \langle f, \beta_{ij} \rangle$$

$$\langle u^N(0), \beta_{ij} \rangle = \langle u_0, \beta_{ij} \rangle \quad \text{for } i,j = 0,1,\ldots, N.$$

Substituting the above expression for u^N, equation (3.2), into (3.3), carrying

out the necessary differentiations, and using the linearity of the inner

product, we arrive at a finite dimensional system of ordinary differential

equations for the Fourier coefficients, $w_{ij}^N(t)$:

(3.4)

$$[A^N \otimes A^N]\dot{W}^N = -(D_1[B^N \otimes A^N]W^N + D_2[A^N \otimes B^N]W^N)$$

$$+ v_1[C^N \otimes A^N]W^N + v_2[A^N \otimes C^N]W^N$$

$$+ \alpha[A^N \otimes A^N]W^N + F^N,$$

$$[A^N \otimes A^N]W^N(0) = E^N,$$

where (recall $B_i = B_i^N$ for each i)

$$A_{ij}^N = \int_0^1 B_i(x)B_j(x)dx, \quad B_{ij}^N = \int_0^1 B_i'(x)B_j'(x)dx,$$

$$C_{ij}^N = \int_0^1 B_i(x)B_j'(x)dx, \quad E_{ij}^N = \int_0^1 \int_0^1 B_i(x)B_j(y)u_0(\gamma)dydx,$$

$$W_{ij}^N = w_{ij}^N(t), \quad \text{and} \quad F_{ij}^N = \int_0^1 \int_0^1 B_i(x)B_j(y)f(\beta)dydx,$$

and $[M \otimes N]$ represents a Kronecker product of matrices. It is important to

note that the entries of the matrices A^N, B^N, and C^N are just the pairwise L^2

inner products on [0,1] of the one-dimensional cubic spline basis elements and

their derivatives; furthermore, the local support properties of cubic splines

guarantee a very nice banded structure for these matrices, in fact they are

hepta-diagonal. We also remark that we have factored the parameters D_i, v_i,

and α out of the inner products in equation (3.3), something we could not do if the coefficients were spatially dependent. However, it will be seen that the computational feature we are trying to illustrate is independent of whether or not the coefficients are constant.

At this point we could rewrite (3.4) in matrix-vector form, but the computational cost of numerically integrating the resulting system would be prohibitive, due both to the size (dimension $= (N+1)^2$) and the sparse nature of the matrices involved. Fortunately however, the action of the Kronecker product $[M \otimes N]$ on any matrix Z turns out to be given by:

$$(3.5) \qquad\qquad [M \otimes N]Z = M \cdot Z \cdot N^t$$

where the multiplication on the right hand side is just ordinary matrix multiplication. Hence the numerical solution of (3.4) requires operation primarily involving the matrices that arise in a one-dimensional cubic spline approximation scheme, namely A^N, B^N, and C^N. Indeed, we have:

$$(3.6) \qquad \begin{aligned} A^N \cdot \dot{w}^N \cdot A^N &= -(D_1 B^N \cdot w^N \cdot A^N + D_2 A^N \cdot w^N \cdot B^N) \\ &\quad + v_1 C^N \cdot w^N \cdot A^N + v_2 A^N \cdot w^N \cdot (C^N)^t + \alpha A^N \cdot w^N \cdot A^N + F^N, \\ A^N \cdot w^N(0) \cdot A^N &= E^N, \end{aligned}$$

where we have used the fact that A^N and B^N are symmetric. It is here that the computational attractiveness of this scheme really becomes apparent because for a given level of approximation N, we compute and store ahead of time the matrices A^N, B^N, C^N, E^N, and F^N in either band or band symmetric mode. Then we call each one up as necessary when we are solving (3.6), taking advantage of their banded structure to speed up the matrix multiplications. Once we solve equation (3.6) (equivalently (3.4)), we can reconstruct the approximate

solution (3.2) and generate a set of "predicted observations" to be compared with the real data. However, before we discuss the computer code that actually integrates (3.6) and produces the Galerkin approximation used in the minimization of the cost functional $J^N(q)$, we describe the modifications to (3.4) and (3.6) that must be made in the presence of variable coefficients [2].

If we include only temporal variation in the parameters, there is little to change, since we can still factor the coefficients out of the inner products in equation (3.3). Taking a linear spline representation for each of the parameters, e.g. $D_1(t) = \sum \delta_k l_k(t)$, $k = 1,2,\ldots,M$, we simply replace D_1, D_2, v_1, v_2, α, β, and γ by their appropriate representations, thus making (3.6) a non-autonomous equation due to the linear spline functions $l_k(t)$. Having solved this time-dependent analogue to equation (3.6) and reconstructed the approximate solution (3.2), we then seek to minimize the cost functional $J^N(\cdot)$ over some finite dimensional set of Euclidean parameters containing the admissible values for the coefficients in the various linear spline representations for D_1, D_2, v_1, v_2, α, β, and γ.

Turning to the case of spatially varying parameters we see that it is not quite so simple to handle because we can now no longer factor the coefficients directly out of the inner products in (3.3). Nevertheless we can preserve the Kronecker product structure and action given by (3.5). More importantly, we will still be able to compute and store ahead of time a set of "inner product matrices", analogous to A^N, B^N, and C^N from (3.4) to be used in the solution of the counterpart to the system (3.6).

As before we take a linear spline representation for each of the parameters, this time in x and y. To illustrate, we examine what happens

to the first term $\langle D_1 u_x^N, (\beta_{ij})_x \rangle$ of equation (3.3). For ease of notation
we assume our coefficients are separable; however we hasten to aid that the
method will still apply in the more general case of non-separable parameter
functions. We write:

$$D_1(x,y) = D_1^x(x) \cdot D_1^y(y) = (\sum \delta_k 1_k(x)) \cdot (\sum \lambda_k 1_k(y)) \quad k = 1, 2, \ldots, M.$$

Substituting in this expression for D_1 and the representation (3.2) for u^N,
differentiating where appropriate, invoking the linearity of the inner
product, and using the separability of the coefficient $D_1(x,y)$, we have that:

$$\{\langle D_1 u_x^N, (\beta_{ij})_x \rangle\} = [B^N(D_1^x) \otimes A^N(D_1^y)] w^N$$

$$= B^N(D_1^x) \cdot w^N \cdot (A^N(D_1^y))^t,$$

where $\quad A_{ij}^N(D_1^y) = \sum \lambda_k \int_0^1 B_i(z) B_j(z) 1_k(z) dz \quad k = 1, 2, \ldots, M$

and $\quad B_{ij}^N(D_1^x) = \sum \delta_k \int_0^1 B_i'(z) B_j'(z) 1_k(z) dz \quad k = 1, 2, \ldots, M.$

In a similar manner we can analyze the changes necessary in the remaining
homogeneous terms of equation (3.3) when the appropriate linear spline
representation is substituted for the parameter appearing in each. In
particular we have that:

$$\{\langle D_2 u_y^N, (\beta_{ij})_y \rangle\} = [A^N(D_2^x) \otimes B^N(D_2^y)] w^N$$

$$= A^N(D_2^x) \cdot w^N \cdot (B^N(D_2^y))^t,$$

$$\{\langle v_1 u^N, (\beta_{ij})_x \rangle\} = [C^N(v_1^x) \otimes A^N(v_1^y)] w^N$$

$$= C^N(v_1^x) \cdot w^N \cdot (A^N(v_1^y))^t,$$

$$\{\langle v_2 u^N, (\beta_{ij})_y \rangle\} = [A^N(v_2^x) \otimes C^N(v_2^y)] w^N$$

$$= A^N(v_2^x) \cdot w^N \cdot (C^N(v_2^y))^t,$$

and $\quad \{\langle \alpha u^N, \beta_{ij} \rangle\} = [A^N(\alpha^x) \otimes A^N(\alpha^y)] w^N$

$$= A^N(\alpha^x) \cdot w^N \cdot (A^N(\alpha^y))^t.$$

Here the matrices $A^N(\cdot)$, $B^N(\cdot)$, and $C^N(\cdot)$ are just linear combinations of the

elementary matrices A_k^N, B_k^N, and C_k^N, whose entries are, in analogy to those of (3.4), the pairwise L^2 inner products on $[0,1]$ of the one-dimensional cubic spline basis elements and their derivatives, now <u>weighted</u> by the kth linear spline, $l_k(\cdot)$, $k = 1,2,\ldots,M$.

We note that it is the convective terms of (3.3) that give rise to the matrices:

$$C^N(\cdot) = \{\sum n_k \int_0^1 B_i(z)B_j'(z)l_k(z)dz\} \qquad k = 1,2,\ldots,M.$$

In addition, we observe that the local support properties of cubic splines again guarantee a nice hepta-diagonal structure to these "weighted inner product matrices"; furthermore for a given level of approximation, N for the state space and M for the parameter space, we can compute and store these matrices ahead of time just as in the simpler constant coefficient case described earlier. We point out, however, that if the inhomogeneous term $f(\beta)$ and the initial condition $u_o(\gamma)$ are non-linear functions of the parameters β and γ, then their respective projections into the subspace H^N (i.e. the matrices E^N and F^N of (3.6)) cannot be computed and stored ahead of time, but rather must be continually updated during the minimization procedure. Nevertheless this needs to be done only at the start of each integration of the approximating system of ordinary differential equations, and the resulting matrices will still exhibit a banded structure. Finally, we note that if temporally and spatially dependent parameters are considered simultaneously, our method still works since we would take a general representation:

$$q(t,x,y) = \sum a_k l_k(t)) \cdot (\sum b_k l_k(x)) \cdot (\sum c_k l_k(y)) \qquad k = 1,2,\ldots,M$$

and then immediately factor the temporal dependence of q out of the inner product and proceed as before.

We now discuss the actual solution of the ordinary differential equation (3.6). Since it is well known that approximation schemes for parabolic partial differential equations often give rise to systems of stiff ordinary differential equations, we use the IMSL code, DGEAR, with its option for stiff systems. As a part of this solution process the general equation $[M \otimes N]Z = Y$, equivalently $M \cdot Z \cdot (N)^t = Y$, must be solved for Z. This task is accomplished by two successive applications of a Cholesky decomposition routine that enables one to solve $FX = G$ for X. In fact one first lets $X = Z \cdot (N)^t$ and solves $MX = Y$ by a Cholesky decomposition of M followed by back-substitution. Then one solves $N \cdot (Z)^t = X^t$ by a Cholesky decomposition of N again followed by back-substitution. The minimization of the cost functional $J^N(q)$ is performed by another standard IMSL code, called ZXSSQ, which employs a modified Levenberg-Marquardt algorithm. The FORTRAN code built around these two large IMSL routines is a modification of an original program written by James Crowley [8]. The testing of this code, which we shall now describe, was performed on the computing system at Brown University running either an IBM 370 or IBM 3081.

In the following examples, we considered a number of "data" sets generated from various known solutions of the constant coefficient model on $\Omega = [0,1] \times [0,1]$:

$$u_t = D(u_{xx} + u_{yy}) + v_1 u_x + v_2 u_y + \alpha u, \quad t>0$$

(3.7) $\quad u(0,x,y) = u_o(x,y)$

$\qquad u(t,x,y) = 0 \quad$ on $\partial\Omega$

Values for D, v_1, v_2, and α were specified, then a simple separation of variables technique was used to calculate each explicit solution. At each of the times $t = .2, .4,$ and $.6$ a matrix of "observations" was then obtained by

evaluating these solutions at the (x,y) grid points x = .1, .3, .5, .7, .9 and y = .1, .3, .5, .7, .9.

We carried out a series of tests on each data set in which various combinations of parameters were considered to be unknown and the remaining parameters held fixed at their true values. Initial guesses of the "unknown" parameters were input into the estimation code and a particular level of approximation specified. The performance of the code could then be assessed in light of factors such as the "error" made in the initial guess, the degree of approximation chosen, or how many parameters were considered unknown. We note that low levels for the state approximations were taken, N = 4,6, or 8. This was done because the computational cost for any given two-dimensional estimation problem far exceeds the cost for a comparable one-dimensional problem (see results of numerical experiments in [1], [2], [3], and [5]). Of course the reason for this is obvious; namely that the two-dimensional setting gives rise to a system (3.6), that consists effectively of $(N + 1)^2$ ordinary differential equations, as opposed to $(N + 1)$ in the one-dimensional case. In fact, just to integrate equation (3.6) for N = 12 takes roughly 12 minutes of CPU time on the IBM 370 and for N = 14 that figure increases to 40 minutes. If the faster IBM 3081 is used, these times decrease to 3 and 10 minutes, but are still very large compared to a one-dimensional problem. Thus, with an eye towards future real-time applications of our estimation technique, we believe it would be fruitful to pursue the implementation of our code on vector machines and other supercomputing processors.

We also remark that the efficiency of the Levenberg-Marquardt minimization algorithm decreases as the number of unknown parameters increases. This is particularly significant if we want to estimate variable coefficients. Indeed, a simple constant coefficient model such as (3.7) has

only four unknown parameters. However, if we take a general transport
equation such as (2.1), and implement the parameter approximation scheme we
have described, then the dimension of the unknown, and in this case
approximate, parameter space will increase dramatically. For example, if we
consider a constant diffusion model with temporally dependent convection and
"growth/death" terms $V_1(t)$, $V_2(t)$, and $\alpha(t)$, and we assume a representation
for each as a linear combination of four linear splines, then we will have
thirteen unknown parameters to search for. Obviously this figure will
increase if we take a linear combination of more than four splines in our
representations; and if we also include spatial dependence in the convection
and "growth/death" terms, then we must deal with an even larger number of
unknown parameters. But the difficulty of minimizing $J^N(\cdot)$ over a large set
of unknowns is not insurmountable, especially in light of recent advances in
computer technology. In fact, as new software (different minimization
routines) and hardware (array and parallel processors) become available, it
is likely that this aspect of this problem can be treated in a relatively
efficient manner.

Example 3.1 We considered the standard heat equation with the diffusion
coefficient, D, equal to 1.0 and the initial condition given by the product of
two one-dimensional "hat" functions. Convergence results were quite good, see
Table 3.1, with no significant improvement in accuracy obtained by increasing
the level of state approximation from $N = 4$ to $N = 8$. However, it is
important to note the dramatic increase in computing expense from the first
case to the second.

Example 3.2 In this example we chose $D = 1.0$, $v_1 = -2.0$, $v_2 = -2.0$, and $\alpha = 19.7392$ in equation (3.7) with $u_0(x,y) = e^x \sin \pi x e^y \sin \pi y$. In the tests summarized in Table 3.2 the level of the state approximation was held at $N = 4$ and it is seen again that the method produced good results.

Example 3.3 For this example we set $D = .20$, $v_1 = -1.0$, $v_2 = -1.8$, and $\alpha = 7.2478$. The relative magnitudes of the coefficients were chosen to reflect a typical example of population dispersal; and to ascertain whether our technique would be able to estimate an asymmetric model (which is almost always the case with real biological data), a directionally dependent convective component, v_1 not equal to v_2, was considered. In Table 3.3 we present a comparison of the method's performance at two levels of state approximation and we see that the parameter estimates were almost all within one-tenth of one percent of the true values. Thus, an improved fit-to-data is obtained at the expense of increased CPU time, but with no great improvement in parameter estimates.

Example 3.4 In this example we considered the problem of estimating parameters in the presence of "noisy" data. We took the same model as in Example 3.3 but introduced random error into the "observations" (see Appendix for details). Representative results are displayed in Table 3.4 and Table 3.5, and together with other tests these suggest that our technique can perform well given data containing noise. It is an interesting qualitative result that in test 3 of Table 3.5 the method me ·ged to estimate the correct relative magnitudes of the true parameters.

Table 3.1

Initial guess	Estimated value N = 4	N = 8	True value	Iterations[1] N=4	N=8	CPU[2](IBM 370) N=4	N=8
1) $D^\circ = .05$	$\bar{D}^4 = 1.0009$	$\bar{D}^8 = 1.0003$	$D = 1.0$	5	4	3 min	18 min
2) $D^\circ = 1.95$	$\bar{D}^4 = 1.0009$	$\bar{D}^8 = 1.0003$	$D = 1.0$	5	4	3 min	18 min

[1]Number of iterations in the minimization algorithm

[2]Computational processing time

Table 3.2

	Initial guess	Estimated value	True value	Iterations	CPU(IBM 370)
1)	$D^o = .50$	$\bar{D}^4 = 1.0003$	$D = 1.0$	14	14.5 min
2)	$v_1^o = -1.0$	$\bar{v}_1^4 = -1.999$	$v_1 = -2.0$	6	9 min
3)	$v_1^o = -.10$	$\bar{v}_1^4 = -1.999$	$v_1 = -2.0$	8	10 min
4)	$v_1^o = -1.0$	$\bar{v}_1^4 = -1.9996$	$v_1 = -2.0$	4	6 min
	$v_2^o = -1.0$	$\bar{v}_2^4 = -1.9996$	$v_2 = -2.0$		
5)	$v_1^o = -1.0$	$\bar{v}_1^4 = -1.9996$	$v_1 = -2.0$	5	7 min
	$v_2^o = -3.0$	$\bar{v}_2^4 = -1.9996$	$v_2 = -2.0$		
6)	$D^o = .50$	$\bar{D}^4 = 1.00001$	$D = 1.0$	13	12 min
	$v_1^o = -1.0$	$\bar{v}_1^4 = -1.9994$	$v_1 = -2.0$		
7)	$D^o = .50$	$\bar{D}^4 = 1.00001$	$D = 1.0$	16	20 min
	$v_1^o = -.10$	$\bar{v}_1^4 = -1.9994$	$v_1 = -2.0$		

$N = 4$

Table 3.3

Initial guess	Estimated value N=4	Estimated value N=8	True value	RSSQ[1] N=4	RSSQ[1] N=8	Iterations N=4	Iterations N=8	CPU(IBM 370) N=4	CPU(IBM 370) N=8
1) $D° = .10$	$\bar{D}^4 = .2003$	$\bar{D}^8 = .20016$	$D = .20$	.6835	5.815×10^{-3}	5	5	4 min	11 min
2) $D° = .10$ $v_2° = -.90$	$\bar{D}^4 = .20056$ $\bar{v}_2^4 = -1.7973$	$\bar{D}^8 = .20017$ $\bar{v}_2^8 = -1.7999$	$D = .20$ $v_2 = -1.8$	.5118	5.68×10^{-2}	7	7	6 min	16 min
3) $D° = .10$ $v_1° = -.50$ $v_2° = -.90$	$\bar{D}^4 = .20057$ $\bar{v}_1^4 = -1.0031$ $\bar{v}_2^4 = -1.7973$	$\bar{D}^8 = .20017$ $\bar{v}_1^8 = -1.0009$ $\bar{v}_2^8 = -1.7994$	$D = .20$ $v_1 = -1.0$ $v_2 = -1.8$	.479	2.268×10^{-3}	9	9	8 min	22 min
4) $\alpha° = 3.6239$	$\bar{\alpha}^4 = 7.2495$	$\bar{\alpha}^8 = 7.246$	$\alpha = 7.2478$	.7399	1.55×10^{-2}	6	6	1 min*	15 min

[1]Residual sum of squares, $J^N(\hat{q})$

*Run on IBM 3081

Table 3.4

	Initial guess	Estimated value	True value	RSSQ	Iterations	CPU(IBM 3081)
1)	$D^o = .10$	$\bar{D}^4 = .2003$	$D = .20$	.6835	5	45 sec
2)	$D^o = .10$	$\bar{D}^4 = .20057$	$D = .20$	.479	9	90 sec
	$v_1^o = -.50$	$\bar{v}_1^4 = -1.0031$	$v_1 = -1.0$			
	$v_2^o = -.90$	$\bar{v}_2^4 = 1.7958$	$v_2 = -1.8$			
3)	$D^o = .10$	$\bar{D}^4 = .2136$	$D = .20$	.4856	8	148 sec
	$v_1^o = -1.5$	$\bar{v}_1^4 = -1.069$	$v_1 = -1.0$			
	$v_2^o = -2.7$	$\bar{v}_2^4 = -1.913$	$v_2 = -1.8$			
	$\alpha^o = 3.6239$	$\bar{\alpha}^4 = 7.848$	$\alpha = 7.2478$			

$N = 4$

Table 3.5
(Noisy data)

	Initial guess	Estimated value	True value	RSSQ	Iterations	CPU(IBM 3081)
1)	$D^o = .10$	$\bar{D}^4 = .1987$	$D = .20$	59.4825	5	45 sec
2)	$D^o = .10$	$\bar{D}^4 = .1982$	$D = .20$	54.2155	9	93 sec
	$v_1^o = -.50$	$\bar{v}_1^4 = -.9628$	$v_1 = 1.0$			
	$v_2^o = -.90$	$\bar{v}_2^4 = -1.8207$	$v_2 = -1.8$			
3)	$D^o = .10$	$\bar{D}^4 = .331$	$D = .20$	54.5492	9	170 sec
	$v_1^o = 1.5$	$\bar{v}_1^4 = -1.6134$	$v_1 = -1.0$			
	$v_2^o = -2.7$	$\bar{v}_2^4 = -3.0303$	$v_2 = -1.8$			
	$\alpha^o = 3.6239$	$\bar{\alpha}^4 = 13.4234$	$\alpha = 7.2478$			

$N = 4$

IV. Parameter estimation in a two-dimensional model of insect dispersal

In a series of mark-recapture experiments, Kareiva recorded the movement of flea beetles along linear arrays of collard patches [10]. A cubic spline based parameter identification technique was subsequently used to analyze this data and to assess the appropriateness of various forms of a general transport equation as models for the observed movement [3], [4], [5]. While this analysis proved quite successful in identifying different mechanisms of dispersal and quantifying their relative importance, it is important to note that the experimental design restricted movement to a one dimensional domain, thus allowing consideration of only one-dimensional transport equations as models. It is apparent of course that a two-dimensional domain provides a more natural setting for most models of insect dispersal (indeed for most models of population dispersal) and in this section we describe the application of our estimation technique to the analysis of cabbage root fly dispersal on a two-dimensional domain.

Our data are taken from mark-recapture experiments by Hawkes in which cabbage root flies (Erioischia brassicae) were related at a point adjacent to and downwind from a cabbage (brassica) crop [9]. Although Wright [16] had rejected anemotaxis as a mechanism of attraction and Thornsteinson [15] claimed "there seems to be no critical evidence that insects orient to plants beyond a few meters", wind tunnel experiments by Coaker and Smith [7] indicated that female E. brassicae do fly upwind in the presence of brassica odor. To resolve this issue Hawkes sought to calculate dispersal rates of E. Brassicae released from a point exposed to brassica odor.

When recapture data suggested random dispersal, an empirical model, $\ln y = a - b\sqrt{x}$, was used to relate the number of flies captured, y, to the distance from the release point, x, where a and b are constants. Average

distances dispersed and thus average rates of dispersal were then calculated on the basis of this model. However, in the case of non-random movement, no such model was available to estimate rates of dispersal. We have subsequently applied our parameter estimation technique to estimate dispersal rates for this type of recapture data, focusing on Hawkes' data for gravid (i.e. egg bearing) female E. brassicae, as this group was observed to exhibit the greatest non-random movement. (We are quick to point out, however, that the applicability of this estimation technique does not depend on any a priori knowledge of a population's specific behavior. Indeed,it is precisely this behavior that we usually wish to ascertain and then analyze).

The experiments were carried out in a large field bordered on the north by a hedge. A 30 by 30 meter cabbage plot was planted immediately south of the hedge with large areas of fallow ground to the south, east, and west of the plot. Water traps spaced six meters apart were placed along the hedge, within the crop, and in the surrounding fallow area as shown in Figure 4.1. Since the prevailing wind direction was from the east-southeast, flies were released from a point at the hedge 24 meters to the west of the northwest corner of the cabbage crop. Direct observation and recapture data showed that movement did not begin until 29.5 hours following the time of initial release. After the onset of dispersal, data representing the distribution of the flies was collected during two consecutive seven hour periods. (For further details of the experiment see Hawkes' paper [9]).

We considered the following two dimensional transport equation as a model for describing the distribution of the flies:

(4.1)
$$u_t = D(u_{xx} + u_{yy}) - v_1(t)u_x - v_2(t)u_y - \alpha(t)u$$
$$(x,y) \; \varepsilon \; [0,1] \times [0,1], \qquad t > 0.$$

Initial data were given by $u(0,x,y) = 0$ for $(x,y) \neq (.5,.5)$ and $u(0,.5,.5) =$ 1930 (the number of marked flies released). Since there were no cabbage plants outside the furthest extent of Hawkes' trap grid, we assumed Dirichlet boundary conditions, $u(t,0,y) = u(t,1,y) = u(t,x,0) = u(t,x,1) \equiv 0$. Here the variables x and y represent dimensionless quantities based on the scaling: $x = \dot{x}$ meters/127.5 meters and $y = \dot{y}$ meters/127.5 meters. Thus the entire field was rescaled to fit on the unit square, with the release point corresponding to $x = y = .5$. The westernmost traps and the easternmost traps corresponded to $y = .3353$ and $y = .9$, respectively, while the northernmost traps (those along the hedge) and the southernmost traps corresponded to $x =$ .5 and $x = .6647$. Time was rescaled as $t = \dot{t}$ hours/24 hours, so that $t_1 =$ .14583 corresponded to the midpoint of the first seven hour census period following the beginning of dispersal and $t_2 = .4375$ corresponded to the midpoint of the second seven hour census period. The convection coefficients, $v_1(t)$ and $v_2(t)$, as well as the "growth/death" term, $\alpha(t)$, were represented by a linear combination of four linear splines. The function $\alpha(t)$ was assumed positive so that the entire negative term $\alpha(t)u$ would reflect the disappearance of flies from the experiment (e.g. through actual death, long range migration, wearing off of the radioactive marker, etc.).

We began our analysis by considering the simpler, constant coefficient equation as a model. Then, by allowing one or more of the coefficients, v_1, v_2, and α, to vary in time, we gradually increased the complexity of the model to arrive at the general equation (4.1). At each stage we sought to minimize the residual sum of squares of differences (RSSQ) between model predictions and observed data. Although it is true that we could have considered the full equation (4.1) from the onset and asked the computer to identify all the

parameters in the model at once, we emphasize that this is not the procedure we followed (see our earlier remarks in Section III regarding the minimization algorithm employed). Instead, we estimated various combinations of parameters while holding the remaining coefficients fixed at certain "nominal" values. As a rule, these were taken to be the "best" values returned from the consideration of a simpler model. For example, to identify the time-dependent profile of the "death" term $\alpha(t)$, we first fixed the diffusion and convection parameters at those values that provided the "best fit" of the constant coefficient model to the recapture data, and then we estimated the "weighting factors", α_k, in the linear spline representation $\alpha(t) = \sum_{k=0}^{3} \alpha_k l_k(t)$. All of the computational work for this analysis was performed on the CDC 6600 computer at Southern Methodist University and the IBM 3081 at Brown University.

In the constant parameter model we sought to estimate the four parameters D, v_1, v_2, and α. This analysis immediately revealed a number of interesting qualitative features (see Table 4.1):

    (1)   a relatively small diffusive term, D;

    (2)   the presence of some directional bias in the convection terms,

        $v_1 < v_2$;

    (3)   the importance of a large "death" term, α.

These results are not surprising, in fact they correlate quite well with what even a casual perusal of the data suggests (see Figure 4.1). There is little evidence of purely random dispersal, indeed some directed movement is almost surely present. Also the fact that only fifty-five out of the original 1930 flies released were recaptured at the first census certainly indicates the need for a large "death" term.

We next introduced temporal variation in the coefficients beginning with the "death" term, $\alpha(t) = \sum_{k=0}^{3} \alpha_k l_k(t)$, where $l_k(t)$ are the standard linear splines as in Sections II and III. The terms D, v_1, and v_2 were held fixed and we sought estimates of the coefficients, α_k, that would lead to a reduction in the RSSQ from the constant parameter model (see Table 4.2). Though we were able to obtain some profiles for $\alpha(t)$ that could be considered biologically plausible, we could not reduce the RSSQ significantly (RSSQ = 200 for the constant coefficient model, RSSQ = 198 for the variable α model). Time varying convection terms were considered next, $v_1(t) = \sum_{k=0}^{3} \beta_k l_k(t)$ and $v_2(t) = \sum_{k=0}^{3} \gamma_k l_k(t)$. But as before, though we obtained some bio-logically arguable profiles for the convection terms (see Table 4.3), we could not reduce the RSSQ. What we did observe consistently was a general intensitivity of the RSSQ to the latter two coefficients in each representation for $v_1(t)$, $v_2(t)$, and $\alpha(t)$. This indicated that our models were simply not predicting the data at the second time point. At this stage it was thought that the diffusion coefficient, though already very small, might nonetheless also exhibit some temporal dependence. Accordingly, some tests were performed to estimate a time varying diffusion term, but still there was no corresponding improvement in the model's prediction of the data (RSSQ remained at 198). In fact, it is interesting to note that for this data set, the total sum of squares, TSSQ, equals 161. This implies that simply using normally distributed noise as a model produced a better fit-to-data than any of the "dynamic" models we had considered so far.

However, these tests were not without value, for they convinced us that our difficulties lay with the magnitude and shape of the variable "death" term, $\alpha(t)$. As a remedy we introduced a discontinuous $\alpha(t)$ into the model with the discontinuity located at the first time point t_1. We retained the

profile of $\alpha(t)$ (taken from earlier testing) from t_0 to t_1, then set $\alpha(t) \approx 0$ for $t > t_1$; in effect "turning off" the "death" mechanism after t_1. The biological interpretation of such a profile is that immediately following the time of release there is a large emigration of the population due to the disturbance of marking and handling [5]. Emigration then settles down to its more "intrinsic" low level, which we artifically took to be zero. It was hoped that this would allow the convective and diffusive mechanisms to redistribute the population over the next time period. In fact, the introduction of this discontinuity resulted in a significant decrease n the RSSQ.

Since we had already determined the purely diffusive component of dispersal to be small, we held the diffusion term fixed at its "best" estimated value from the constant coefficient model testing. We also held the "death" function fixed at the discontinuous profile described above. By estimating various combinations of the coefficients β_k and γ_k in the representations of the terms v_1 and v_2, we were able to produce convection profiles that reduced the RSSQ to a value of 98 (see Table 4.4). In light of this result, the insensitivity of the RSSQ to α_i, β_i, and γ_i, $i = 2,3$, in the expressions for v_1, v_2, and α can be understood. Before the introduction of the discontinuous "death" term, the very large value of $\alpha(t)$ at t_1 influenced the model's behavior for a significant amount of time after t_1 (even if $\alpha_2 = \alpha_3 = 0.0$). This large value dominated the mechanisms of dispersal and caused the model to predict a population identically equal to zero at the second time point, t_2, regardless of the profiles of the convection terms. Only by "turning off the decay", via the discontinuity, could we allow for convection to be identified as a significant component of the motion (see Figure 4.2).

Having produced a model which allowed more freedom to the dispersive mechanisms, we proceeded to carry out a set of tests to try to "fine tune" the convective terms. Since some of the profiles that we had estimated yielded a good RSSQ but made little biological sense, we sought to estimate more biologically reasonable convection functions. The results depicted in Table 4.5 show that our attempts met with qualified success. While the qualitative feature of decreasing x-convection and increasing y-convection that we identified can be explained by the greater proximity of the cabbage crop to the release point when measured in the x-direction than when measured in the y-direction, we are quick to note that this set of profiles did not significantly reduce the RSSQ from its previous best minimum value of 98. In fact, we actually identified several sets of convection functions during our analysis that produced this value for the RSSQ. Such an example of non-uniqueness is of course not unexpected, being a reflection of the inherent "ill-posedness" of many inverse problems of this type.

We also performed tests to try to "fine tune" the variable "death" term. Recognizing the artificial nature of the discontinuity introduced in $\alpha(t)$, we sought to identify a profile for $\alpha(t)$ with a steep gradient in a neighborhood of the first time point t_1. Here we considered the representation $\alpha(t) = \sum_{k=0}^{11} \alpha_k 1_k(t)$ and set $\alpha_0 \equiv \alpha_1$ and $\alpha_4 \equiv \alpha_5 \equiv \alpha_6 \equiv \ldots \equiv \alpha_{11}$. We then estimated the "weighting factors" α_1, α_2, α_3, and α_4. The results are displayed in Table 4.6 and we see the presence of a very steep gradient in the estimated profile for $\alpha(t)$.

Finally, we have performed a series of tests to identify spatial dependence in the convection terms. We assumed the representations

$$v_1(t,x) = (\sum_{k=0}^{3} \beta_k 1_k(t)) \cdot (\sum_{k=0}^{3} \zeta_k 1_k(x)) \text{ and } v_2(t,y) = (\sum_{k=0}^{3} \gamma_k 1_k(t)) \cdot (\sum_{k=0}^{3} \eta_k 1_k(y))$$

where the coefficients β_k and γ_k were set identically equal to 1.0 so that purely spatial variation in convection was considered. Our estimation algorithm was then applied to the "weighting factors" ζ_k and η_k, see Table 4.7. Next, using the resulting spatially dependent profiles, new estimates were sought for the parameters β_k and γ_k defining the temporally dependent portions of convection, see Table 4.8. We caution, however, that while the inhomogeneity of the experimental site certainly suggests that we consider spatial dependence in the convective terms, the experimental feature of a single point release does not allow the proper separation of temporal effects on convection from spatial effects. So while we actually succeeded in lowering the RSSQ to 92.42 (see Table 4.7) and subsequently to 89.68 (see Table 4.8), it is not clear that our data can support these results.

We turn now to a discussion of a statistical criterion which we used to help evaluate the relative strengths of our models. Following the method described in [4] and [5] (an ad hoc modification of multiple regression analyses and significance tests based on the F-distribution), we calculated F-statistics comparing the variation explained by a particular model, TSSQ − RSSQ, with the unexplained variation, RSSQ. The degrees of freedom for these two quantities were taken to be k and (n − k − 1), respectively, where k equals the number of unknown parameters in the given model and n equals the number of data points. Hence, recalling that the TSSQ for our data set is 161, we see that the percent of the TSSQ explained by our "best" model, (TSSQ − RSSQ)/TSSQ, is 39.3%, with a corresponding F-statistic, $F_{13, \, 74} = 3.72$ at a significance level, $p < .001$. We note that in general the F-statistic can also be used (albeit in an ad hoc manner) to measure the significance of reductions in the RSSQ induced by adding parameters to a model, see [4] and [5]. Indeed, we are tempted to use this statistic to assess the relative

importance of different mechanisms of dispersal in our model for the cabbage

root flies. (After all, this was one of the motivations for Hawkes'

experiment). Unfortunately, the fit-to-data of our early models was so poor

that such a use was precluded. In fact, we observe that since the calculation

of such statistics requires that TSSQ > RSSQ, F-tests could not be applied to

the models of Tables 4.1, 4.2, and 4.3. This is because all of the testing

through that stage had resulted in values for the RSSQ that always exceeded

198, whereas we had computed the TSSQ to be 161. However, as we have seen, we

subsequently identified a model, which provided not only a statistically

significant explanation of the total sum of squares error, but more

importantly, a biologically meaningful explanation of the data in terms of

diffusive, convective, and "growth/death" mechanisms of dispersal.

We close this section with a brief discussion of some issues which our

analysis raised concerning experimental design and the data that results. A

characteristic feature of dispersal experiments is the use of a point release

of the initial population. While such a technique certainly facilitates the

actual execution of an experiment, any subsequent mathematical analysis must

deal with the problem of approximating a "delta function" for use as initial

data. But, more basic than a purely mathematical consideration, it has been

suggested that point releases give rise to data that over-represent the region

immediately surrounding the release site and under-represent the more distant

regions [5], thus masking the effect of any possible convective mechanism.

Furthermore, for the particular experiment we considered, the use of a point

release had an additional impact. Because the release point was located at

the edge of the array of traps, fully half of the initial population was lost

from the model almost instantaneously. As a remedy it would seem very

reasonable to try to effect a distributed release of the initial population, and to do so within the central regions of the array.

Table 4.1

Constant parameter model

1)   D and α searched; $v_1 = v_2 = 0.0$, held fixed

   Estimated: $D = 349.103$

                 $\alpha = 51.716$

   RSSQ = 387.98

2) v_1, v_2, and α searched; $D = 349.103$, held fixed

   Estimated: $v_1 = 14.915$

                 $v_2 = 39.618$

                  $\alpha = 52.933$

   RSSQ = 308.31

3) v_1, v_2, and α searched; $D = 3.49103$, held fixed*

   Estimated: $v_1 = 14.148$

                 $v_2 = 31.598$

                  $\alpha = 59.551$

   RSSQ = 200.63

$[D] = m^2/day$, $[v_1] = [v_2] = m/day$, $[\alpha] = day^{-1}$

N=4

----

*Note the reduction of D by two orders of magnitude. Subsequent reductions did not lower the RSSQ.

Table 4.2

Time varying "growth/death" term added,

D, v_1, and v_2 held fixed at final values from Table 4.1

1) α_k, $k = 0, 1, 2, 3$ searched

   Estimated: $\alpha_0 = 59.551$

   $\alpha_1 = 59.555$

   $\alpha_2 = 21.939$

   $\alpha_3 = 154.200$

   RSSQ = 200.35

2) α_k, $k = 0, 1$ searched; $\alpha_k = 1.0$, $k = 2, 3$ held fixed

   Estimated: $\alpha_0 = 67.773$

   $\alpha_1 = 51.605$

   RSSQ = 197.98

$[\alpha_k] = \text{day}^{-1}$

N=4

Table 4.3

Time varying convection terms added,

D and $\alpha(t)$ held fixed at final values from Table 4.2

1) β_k, γ_k, k = 2,3 searched; β_k, γ_k, k = 0, 1 held fixed at final values

for v_1 and v_2 from Table 4.1

        Estimated: β_2 = 1007.704

                           β_3 = 282.792

                           γ_2 = 1272.759

                           γ_3 = 23.053

        RSSQ = 196.99

2) β_j, j = 0, 1, 2, 3 searched; $\gamma_j = 2\beta_j$

        Estimated: β_0 = 14.148

                           β_1 = 14.148

                           β_2 = 13.501

                           β_3 = 48.060

        RSSQ = 197.79

3) β_k, γ_k, k = 0, 1 searched; $\beta_k = 1/2\beta_1$ and $\gamma_k = 1/2\gamma_1$, k = 2,3

        Estimated: β_0 = 14.148

                           β_1 = 14.148

                           γ_0 = 31.598

                           γ_1 = 31.598

        RSSQ = 197.69

$[\beta_k] = [\gamma_k]$ = m/day

N=4

Table 4.4

Discontinuous "growth/death" term introduced,

$\alpha(t)$ held fixed with a discontinuous profile

1) β_k and γ_k, $k = 0$, 1, searched; $D = 3.49$ fixed, $\beta_k = 1/2\beta_1$ and $\gamma_k = 1/2\gamma_1$, $k = 2,3$

Estimated: $\quad \beta_0 = 14.148$

$\beta_1 = 14.148$

$\gamma_0 = 31.598$

$\gamma_1 = 31.598$

RSSQ = 168.63

2) β_k and γ_k, $k = 2$, 3 searched; $D = 3.49$ fixed, β_k and γ_k, $k = 0$, 1 held fixed at final values for v_1 and v_2 from Table 4.1

Estimated: $\quad \beta_2 = 504.519$

$\beta_3 = 1269.616$

$\gamma_2 = 14.801$

$\gamma_3 = 411.220$

RSSQ = 98.11

3) β_k and γ_k, $k = 0$, 1 searched; $D = 3.49$ fixed, β_k and γ_k, $k = 2,3$ held fixed at values from test 2 above

Estimated: $\quad \beta_0 = 14.148$

$\beta_1 = 14.148$

$\gamma_0 = 31.598$

$\gamma_1 = 31.598$

RSSQ = 98.00

4)   D, β_0 and γ_0 searched; $\beta_1 = \beta_0$, $\gamma_1 = \gamma_0$, β_k and γ_k, $k = 2$, 3 held fixed as before

Estimated: $D = 3.49$

$\beta_0 = 14.148$

$\gamma_0 = 31.598$

RSSQ = 98.00

$[D] = m^2/day$, $[\beta_k] = [\gamma_k] = m/day$, $[\alpha_k] = day^{-1}$

N=4

Table 4.5

"Fine tuning" of convection terms,

$D = 3.49$ and $\alpha(t)$ held fixed at a discontinuous profile

1) β_k and γ_k, $k = 2, 3$ searched; $\beta_k = \gamma_k = 31.6$, $k = 0, 1$ held fixed

     Estimated: $\beta_2 = 4.07$

                     $\beta_3 = 88.5$

                     $\gamma_2 = 75.68$

                     $\gamma_3 = 325.48$

     RSSQ = 105.00

2) β_2 and β_3 searched; all other coefficients held fixed at values from test 1

     Estimated: $\beta_2 = 3.424$

                     $\beta_3 = 4.143$

     RSSQ = 100.37

3) β_2 and β_3 searched; $\beta_0 = \beta_1 = 14.148$ and remaining coefficients held fixed at values from test 1

     Estimated: $\beta_2 = 11.01$

                     $\beta_3 = .364$

     RSSQ = 97.73

$[D] = m^2/day$, $[\beta_k] = [\gamma_k] = m/day$, $[\alpha_k] = day^{-1}$

$N=4$

Table 4.6

Final values of parameters for the "best" model

with a continuous $\alpha(t)$

$D = 3.49 \text{ m}^2/\text{day}$

$v_1(t) = \sum_{k=0}^{3} \beta_k l_k(t)$, where

$\beta_0 = 14.15 \text{ m/day}$

$\beta_1 = 14.15 \text{ m/day}$

$\beta_2 = 11.01 \text{ m/day}$

$\beta_3 = .364 \text{ m/day}$

$v_2(t) = \sum_{k=0}^{3} \gamma_k l_k(t)$, where

$\gamma_0 = 31.6 \text{ m/day}$

$\gamma_1 = 31.6 \text{ m/day}$

$\gamma_2 = 75.68 \text{ m/day}$

$\gamma_3 = 325.48 \text{ m/day}$

$\alpha(t) = \sum_{k=0}^{11} \alpha_k l_k(t)$, where

$\alpha_0 = \alpha_1$ and $\alpha_4 = \alpha_5 = \alpha_6 = \cdots = \alpha_{11}$ and

$\alpha_1 = 67.773 \text{ day}^{-1}$

$\alpha_2 = 67.773 \text{ day}^{-1}$

$\alpha_3 = 61.804 \text{ day}^{-1}$

$\alpha_4 = .003 \text{ day}^{-1}$

RSSQ = 104.71

Table 4.7

Spatial dependence considered in the convection terms,

D and $\alpha(t)$ held fixed as in Table 4.6

$$v_1(x) = \sum_{k=0}^{7} \zeta_k 1_k(x)$$

$$v_2(y) = \sum_{k=0}^{7} \eta_k 1_k(y)$$

Estimated:		Estimated:	
$\zeta_0 = 11.851$		$\eta_0 = 10.685$	
$\zeta_1 = 11.871$		$\eta_1 = 19.114$	
$\zeta_2 = 16.222$		$\eta_2 = 44.514$	
$\zeta_3 = 16.152$		$\eta_3 = 37.451$	
$\zeta_4 = .673$		$\eta_4 = 107.270$	
$\zeta_5 = .885$		$\eta_5 = 88.090$	
$\zeta_6 = 34.978$		$\eta_6 = 105.171$	
$\zeta_7 = 35.306$		$\eta_7 = 65.052$	

RSSQ = 92.42

$[\zeta_k] = [\eta_k] = $ m/day

N=4

Table 4.8

Temporal dependence in convection terms

re-estimated based on results from Table 4.7

$$v_1(t,x) = (\sum_{k=0}^{3} \beta_k l_k(t)) \cdot v_1(x) \qquad v_2(t,y) = (\sum_{k=0}^{3} \gamma_k l_k(t)) \cdot v_2(y)$$

Estimated: $\beta_0 = 1.000$ Estimated: $\gamma_0 = 1.001$

$\beta_1 = .998$ $\gamma_1 = 1.000$

$\beta_2 = 2.425$ $\gamma_2 = 1.222$

$\beta_3 = 2.519$ $\gamma_3 = 1.455$

RSSQ = 89.68

$[\beta_k] = [\gamma_k] = m/day$

N=4

Figure 4.1

First census:

```
                              - y -

2     2     3     1     6     4     3     3           1
*     *     *     *  x  *     *     *     *     *     *     *     *     *


      2           1     2     4     3     2     2     *     *     *     *
*     *     *     *     *     *     *     *     *     *     *     *     *


      2     1     1           1     1           4     1     1           1
*     *     *     *     *     *     *     *     *     *     *     *     *


|
x                                                *     *     *     *     1
|                                                                        *
```

fallow   crop

Second census:

```
                              - y -

                  2           3     1     1     1     2     4     2
*     *     *     *  x  *     *     *     *     *     *     *     *     *


            1     1     1     2           3     4     2     2     4
*     *     *     *     *     *     *     *     *     *     *     *     *


                        1     1     1     3     3     1     2     3
*     *     *     *     *     *     *     *     *     *     *     *     *


|
x                                                *     *     *     3     1
|                                                                  *     *
```
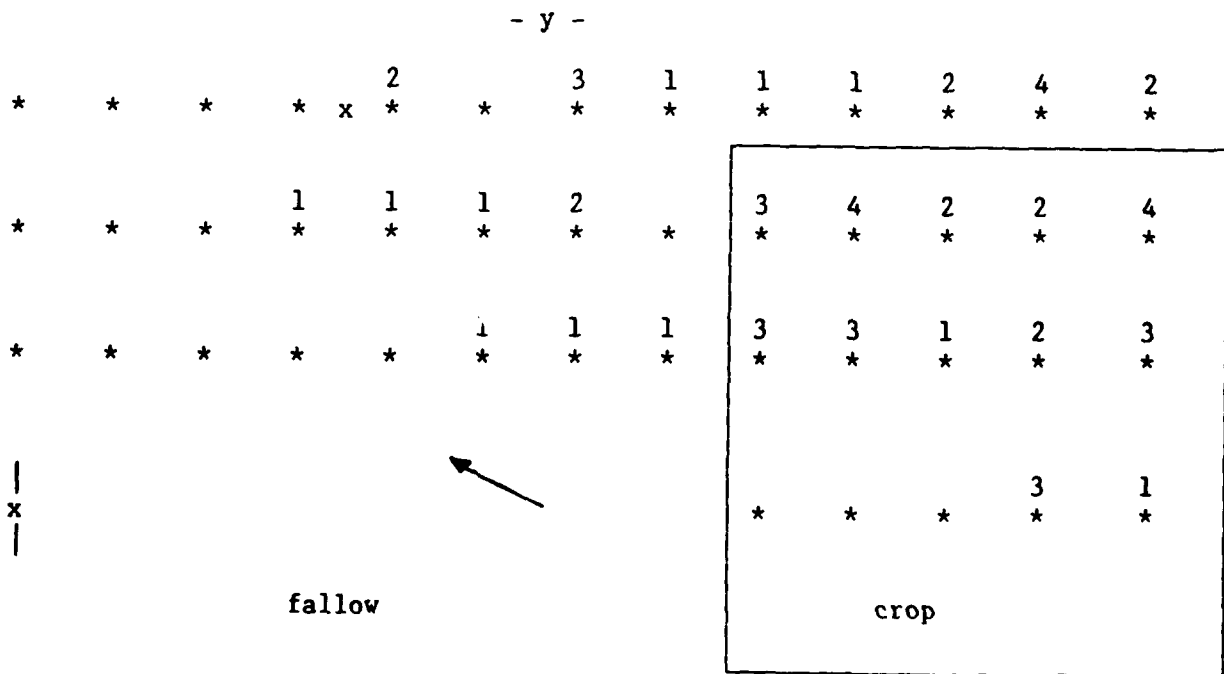
fallow   crop

The cross marks the release point and the arrow indicates the .ind direction.

Figure 4.2
Residual error at each grid point

First census:

- y -

```
-.98 -.51 -1.09  1.22      -3.67 -1.78 -1.03 -1.38  1.22  -.13   .51   .25   .08
  *    *    *     *    x    *     *     *     *     *    *     *     *     *

 .99 -.56  1.86  1.16       .27  -1.84 -1.08  -.43| -.81   .81   .49   .25   .07
  *    *    *     *          *     *     *     *  |  *     *     *     *     *

 .88 -.71   .66   .92      2.02    .93   .71   1.4| 2.92  -.28  -.56   .22  -.93
  *    *    *     *          *     *     *     *  |  *     *     *     *     *

  |                                               |  .76   .56   .32   .16  -.95
  x                          ←                    |  *     *     *     *     *
  |
              fallow                                         crop
```

Second census:

- y -

```
-.09   .02   .18   .37      -1.46   .7   -2.13   .09   .38   .79   .25  -1.43   .5
  *     *     *     *   x     *     *     *      *     *     *     *     *     *

-.09   .02   .18  -.63      -.46   -.3   -1.13  1.09| -1.62 -2.21   .25       .57 -1.49
  *     *     *     *   x     *     *     *      *  |   *     *     *         *     *

-.08   .01   .17   .34       .5    -.35   -.2    .01| -1.72 -1.35  1.08       .37  -.69
  *     *     *     *          *     *     *      *  |   *     *     *         *     *

  |                                                 |   .98   1.26  1.6     -1.18   .78
  x                          ←                      |   *     *     *        *     *
  |
              fallow                                           crop
```

The cross marks the release point and the arrow indicates the wind direction.

RSSQ = 97.73

Appendix

Introduction of Random Error into Data

We describe how we introduced random error into our data so that the estimation scheme could be tested in the presence of "noise". We first used the IMSL routine GGNML to produce a set of normal random numbers with mean 0 and variance 1 to correspond to our set of analytically generated data. Using these random numbers we perturbed the data points with the requirement that the errors remain less than ten percent with 95% probability. That is, we treated each data point as the mean of a normal distribution, then adjusted the variance to insure that 1.96 standard deviations from the mean corresponded to a ten percent deviation from the true value.

References

1. H.T. Banks, J.M. Crowley and K. Kunisch, Cubic spline approximation techniques for parameter estimation in distributed systems, IEEE Trans. Auto. Control, 28(7), (1983), 773-786.

2. H.T. Banks and P.L. Daniel, Estimation of variable coefficients in parabolic distributed systems, IEEE Trans. Auto Control, 30(4), (1985), 386-398.

3. H.T. Banks, P.L. Daniel and P. Kareiva, Estimation techniques for transport equations, LCDS Tech. Rep. 83-23, July, 1983, Brown University; Mathematics in Biology and Medicine, Lecture Notes in Biomathematics, 57(1985), New York: Springer-Verlag, p. 428-438.

4. H.T. Banks and P. Kareiva, Parameter estimation techniques for transport equations with application to population dispersal and tissue bulk flow models, Journal of Mathematical Biology, 17(1983), 253-273.

5. H.T. Banks, P. Kareiva and P.K. Lamm, Modeling insect dispersal and estimating parameters when mark-release techniques may cause initial disturbances, Journal of Mathematical Biology, 22(1985), 259-277.

6. H.T. Banks and K. Murphy, Estimation of coefficients and boundary parameters in hyperbolic systems, LCDS Tech. Rep. 84-5, February, 1984, Brown University; SIAM J. Contr. Optimiz., 24(1986), 926-950.

7. T.H. Coaker and J.L. Smith, Behavior of the adult cabbage root fly, Natn. Veg. Res. Stn. Rep., 1969, 87-88.

8. J.M. Crowley, Numerical Methods of Parameter Identification for Problems Arising in Elasticity, Ph.D. Thesis, Brown University, May, 1982.

9. C. Hawkes, Dispersal of adult cabbage root fly (Erioischia brassicae (Bouche)) in relation to a brassica crop, Journal of Applied Ecology, 11(1), (1974), 83-93.

10. P. Kareiva, Experimental and mathematical analyses of herbivore movement: quantifying the influence of plant spacing and quality of foraging discrimination, Ecological Monographs, 52(3), (1982), 261-282.

11. K. Kunisch and L. White, The parameter estimation problem for parabolic equations in multidimensional domains in the presence of point evaluations, SIAM J. Contr. Optimiz., 23(1985), 900-927.

12. J.L. Lions, Optimal Control of Systems Governed by Partial Differential Equations, New York: Springer-Verlag, 1971.

13. A. Okubo, Diffusion and Ecological Problems: Mathematical Models, Berlin: Springer-Verlag, 1980.

14. M.H. Schultz, Spline Analysis, Englewood Cliffs, N.J.: Prentice-Hall, 1973.

15. A.J. Thornsteinson, Host selection in phytophagous insects, <u>Annual Review of Entomology</u>, 5(1960), 193-218.

16. R.H. Wright, The olfactory guidance of flying insects, <u>Canadian Entomologists</u>, 90(1958), 81-89.

17. L.L. Zia, Parameter Estimation Techniques for Two-Dimensional Transport Equations with Application to Models of Insect Dispersal, Ph.D. Thesis, Brown University, May, 1985.

END

8-87

DTIC